Available online at www.sciencedirect.com
ScienceDirect
Nuclear Medicine and Biology 36 (2009) 155–162
NUCLEAR MEDICINE — AND — BIOLOGY
www.elsevier.com/locate/nucmedbio

Preparation and evaluation of ethyl [^{18}F]fluoroacetate as a proradiotracer of [^{18}F]fluoroacetate for the measurement of glial metabolism by PET

Tetsuya Mori[a], Li-Quan Sun[a,b], Masato Kobayashi[a], Yasushi Kiyono[a,*], Hidehiko Okazawa[a], Takako Furukawa[a], Hidekazu Kawashima[c], Michael J. Welch[d], Yasuhisa Fujibayashi[a]

[a]*Biomedical Imaging Research Center, University of Fukui, Fukui 910-1193, Japan*
[b]*School of Life Science and Technology, Beijing Institute of Technology, Beijing 100081, China*
[c]*Graduate School of Medicine, Kyoto University, Kyoto 606-8501, Japan*
[d]*Mallinckrodt Institute of Radiology, Washington University School of Medicine, St. Louis, MO 63110, USA*

Received 3 October 2008; received in revised form 5 November 2008; accepted 11 November 2008

Abstract

Introduction: Changes in glial metabolism in brain ischemia, Alzheimer's disease, depression, schizophrenia, epilepsy and manganese neurotoxicity have been reported in recent studies. Therefore, it is very important to measure glial metabolism in vivo for the elucidation and diagnosis of these diseases. Radiolabeled acetate is a good candidate for this purpose, but acetate has little uptake in the brain due to its low lipophilicity. We have designed a new proradiotracer, ethyl [^{18}F]fluoroacetate ([^{18}F]EFA), which is [^{18}F]fluoroacetate ([^{18}F]FA) esterified with ethanol, to increase the lipophilicity of fluoroacetate (FA), allowing the measurement of glial metabolism.
Methods: The synthesis of [^{18}F]EFA was achieved using ethyl *O*-mesyl-glycolate as precursor. The blood–brain barrier permeability of ethyl [1-^{14}C]fluoroacetate ([^{14}C]EFA) was estimated by a brain uptake index (BUI) method. Hydrolysis of [^{14}C]EFA in the brain was calculated by the fraction of radioactivity in lipophilic and water fractions of homogenized brain. Using the plasma of five animal species, the stability of [^{14}C]EFA was measured. Biodistribution studies of [^{18}F]EFA in ddY mice were carried out and compared with [^{18}F]FA. Positron emission tomography (PET) scanning using common marmosets was performed for 90 min postadministration. At 60 min postinjection of [^{18}F]EFA, metabolite studies were performed. Organs were dissected from the marmosets, and extracted metabolites were analyzed with a thin-layer chromatography method.
Results: The synthesis of [^{18}F]EFA was accomplished in a short time (29 min) and with a reproducible radiochemical yield of 28.6±3.6% (decay corrected) and a high radiochemical purity of more than 95%. In the brain permeability study, the BUI of [^{14}C]EFA was 3.8 times higher than that of sodium [1-^{14}C]fluoroacetate. [^{14}C]EFA was hydrolyzed rapidly in rat brains. In stability studies using the plasma of five animal species, [^{14}C]EFA was stable only in primate plasma. Biodistribution studies in mice showed that the uptake of [^{18}F]EFA in selected organs was higher than that of [^{18}F]FA. From nonprimate PET studies, [^{18}F]EFA was initially taken into the brain after injection. Metabolites related to the tricarboxylic acid (TCA) cycle were detected in common marmoset brain.
Conclusion: [^{18}F]EFA rapidly enters the brain and is then converted into TCA cycle metabolites in the brains of common marmosets. [^{18}F]EFA shows promise as a proradiotracer for the measurement of glial metabolism.

Keywords: [^{18}F]Fluoroacetate; Ethyl [^{18}F]fluoroacetate; Proradiotracer; Glial metabolism; PET

1. Introduction

There is now a growing body of evidence indicating that glial cells, particularly astrocytes, contribute actively to synapse development, synaptic transmission and neuronal excitability [1–4]. Furthermore, changes in glial metabolism in brain ischemia [5,6], Alzheimer's disease [7], depression [8], schizophrenia [9], epilepsy [10] and manganese neurotoxicity [11] have been reported. Therefore, it is very important to measure glial metabolism in vivo for the elucidation and diagnosis of these diseases.

For this purpose, a positron emission tomography (PET) tracer for measuring glial metabolism should provide useful

* Corresponding author. Tel.: +81 776 61 8420; fax: +81 776 61 8170.
E-mail address: ykiyono@u-fukui.ac.jp (Y. Kiyono).

0969-8051/$ – see front matter © 2009 Elsevier Inc. All rights reserved.
doi:10.1016/j.nucmedbio.2008.11.006

information. Radioactive carbon-labeled acetate has been used for glial metabolism studies in basic research because exogenous acetate is selectively taken up by astrocytes via monocarboxylic acid transporter-1 and is converted into acetyl-CoA in the cells [12,13]. However, the brain uptake of acetate from the blood stream is very low due to low lipophilicity.

To resolve this problem, two approaches have recently been reported. One approach using [1-^{11}C]octanoate has been reported by Kuge et al. [14,15] and Yamazaki et al. [16] Their strategy was to use high lipophilic fatty acid for blood–brain barrier (BBB) permeability and to measure β-oxidation activity in astrocytes. Another approach was a proradiotracer concept reported by Inoue et al. [17] and Momosaki et al. [18] Their strategy involved combining radiolabeled acetate with a highly lipophilic group for BBB permeability, and then this proradiotracer is cleaved to radiolabeled acetate and the lipophilic group in the brain by carboxyesterase. However, both approaches have limited use because both compounds were labeled with carbon-11 (half-life, 20 min).

We have designed a new proradiotracer, ethyl [^{18}F]fluoroacetate ([^{18}F]EFA), which is esterified [^{18}F]fluoroacetate ([^{18}F]FA) with ethanol (Fig. 1). [^{3}H]Fluoroacetate has been reported to accumulate selectively in glia and has been proposed as potential tracer for glial oxidative metabolism [12]. Fluoroacetate (FA) has been extensively used in brain metabolism studies as a specific inhibitor of glial cell metabolism [19,20]. Moreover, Hassel et al. [21] demonstrated that FA did not inhibit neuronal tricarboxylic acid (TCA) cycles, but inhibited glial TCA cycles in mice using nuclear magnetic resonance spectroscopy and gas chromatography/mass spectroscopy. Therefore, FA is considered to be selectively transported into the glial metabolic compartment and converted into fluoroacetyl-CoA and 2-fluorocitrate in TCA cycles [12,20,22]. Fluorine-18 has a half-life (110 min) longer than that of carbon-11, is more convenient for the synthesis and metabolism studies of PET radiopharmaceuticals, and can also able be applied commercially [23].

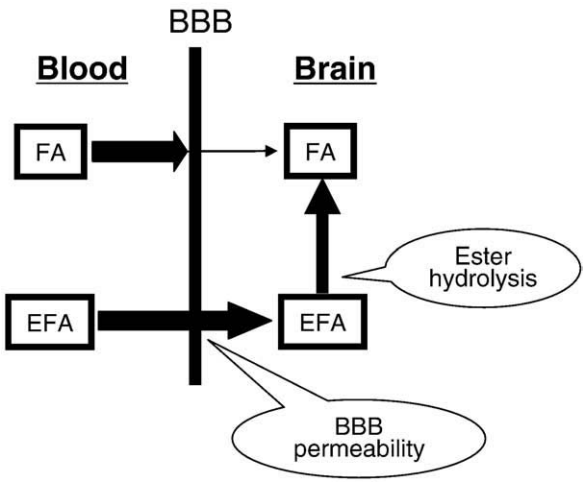

Fig. 1. The concept of a proradiotracer of [^{18}F]FA for assessing glial metabolism in the brain. FA: fluoroacetate; EFA: ethyl fluoroacetate.

In this study, the possibility of [^{18}F]EFA as a proradiotracer for the measurement of glial metabolism was assessed by investigating membrane permeability, ester hydrolysis in the brain and plasma, and PET imaging in common marmosets.

2. Materials and methods

2.1. Reagents, instruments and materials

All chemicals were obtained from commercial sources and used without further purification. The following labeled compounds, ethyl [1-^{14}C]fluoroacetate ([^{14}C]EFA), [1-^{14}C]fluoroacetate ([^{14}C]FA) and [^{3}H]H_2O, were purchased from American Radiolabeled Chemicals, Inc. (St. Louis, MO, USA), and [1,5-^{14}C]citrate and [1-^{14}C]acetyl-CoA were purchased from Amersham Biosciences, Inc. (UK). Ethyl glycolate and methanesulfonyl chloride were obtained from Tokyo Kasei Kogyo Co. Ltd. (Tokyo, Japan). Ethyl fluoroacetate, as reference standard, was purchased from Wako Pure Chemical Industries, Ltd. (Tokyo, Japan). Potassium carbonate, sodium hydroxide, anhydrous magnesium sulfate, hydrochloric acid, anhydrous acetonitrile and methylene chloride were purchased from Sigma-Aldrich Japan KK (Tokyo, Japan). Triethylamine and sodium bicarbonate were purchased from Kanto Kagaku (Osaka, Japan). Ethanol [99.5% for high-performance liquid chromatography (HPLC)] was purchased from Nacalai Tesque, Inc. (Kyoto, Japan). Sep-Pak cartridges were purchased from Waters Corporation (Milford, MA, USA).

Analytical HPLC was performed on a Waters Corporation 600E system equipped with Waters 490E programmable multiwavelength UV detector set at 210 nm and a Bioscan Flow counter (Washington, DC, USA). A reversed-phase Hydrosphere C_{18} column (4.6×150 mm; YMC, Kyoto, Japan) was used with ethanol/H_2O (10:90) as mobile phase at a flow rate of 1.0 ml/min. Radio thin-layer chromatography (TLC) was performed using 0.25-mm Silica Gel 60 Sheets F_{254} purchased from Nacalai Tesque, Inc.

Plasma from rats and rabbits was obtained from Sankyo Labo Service Co. (Tokyo, Japan), and dog plasma was acquired from NARC Co. (Chiba, Japan). Common marmosets (*Callithrix jacchus*) weighting 340–390 g were obtained from Japan SLC, Inc. (Shizuoka, Japan), and plasma was prepared from fresh whole blood. Human plasma was prepared from fresh whole blood provided by a healthy volunteer.

Wistar rats and ddY mice were purchased from Sankyo Labo Service Co. and maintained in a specific pathogen-free room. Common marmosets were housed in stainless-steel cages in a temperature-controlled (28±2°C) and humidity-controlled (50±10%) animal room and fed a balanced

marmoset diet (CMS-1; CLEA Japan, Inc., Tokyo, Japan) with free access to water. Animal experiments were carried out in accordance with the Institutional Guidelines for the Care and Use of Experimental Animals and approved by the internal ethical committees of the Department of Medicine, University of Fukui.

2.2. Preparation of no-carrier-added [^{18}F]EFA and [^{18}F]FA

Synthesis of [^{18}F]EFA was performed using a simple instrument set-up, as shown in Fig. 2A. In this reaction, ethyl *O*-mesyl-glycolate was synthesized first, then it was used as precursor (Fig. 2B) [23]. No-carrier-added [^{18}F] fluoride was produced via the ^{18}O(p,n) ^{18}F reaction in a Siemens RDS eclipse cyclotron (11 MeV protons) on an enriched water target. No-carrier-added aqueous [^{18}F] fluoride (1.35 ml; 3.7 GBq) was added onto a Sep-Pak Acell QMA Light cartridge, which was converted into CO_3^{2-} form by treatment of an aqueous solution of 0.1 M K_2CO_3. Almost all [^{18}F]fluoride anions were extracted from [^{18}O] water and trapped by the cartridge, and the enriched [^{18}O] water was recovered in the reservoir. Half a milliliter of 16.7 mM aqueous potassium carbonate solution was employed to elute the trapped [^{18}F]fluoride anion from the QMA cartridge. The eluate with [^{18}F]fluoride solution was introduced to the reaction vessel. The solution of 16.4 mg of Kryptofix 2.2.2 dissolved in 1 ml of anhydrous acetonitrile was then added to the reaction vessel. Water in the mixture was azeotropically evaporated three times at 95°C with nitrogen gas flow and anhydrous acetonitrile (500 μl×3). After the drying step, 2.9 mg of ethyl *O*-mesyl-glycolate dissolved in 1 ml of anhydrous acetonitrile was added to the residue in the reaction vessel. The labeling reaction was maintained at 105°C for 5 min in the closed-reaction vessel to give rise to [^{18}F]EFA. Then, the reaction solvent anhydrous acetonitrile was removed at 95°C with nitrogen gas flow. After 5 min, the residue in the reaction vessel was distilled under reduced pressure (about 14 mmHg), and the distillate [^{18}F]EFA was collected and trapped by 1 ml of ice-cold ethanol (99.5%) in a 3-ml vial. Finally, the ethanol solution was transferred through a Sep-Pak Alumina N Plus cartridge and further filtered by a 0.22-μm sterile filter. The product was analyzed by TLC and HPLC. When animal experiments were performed, the final product was diluted with saline to 5% ethanol solution. The preparation of [^{18}F]FA was performed as described previously by Sun et al. [23].

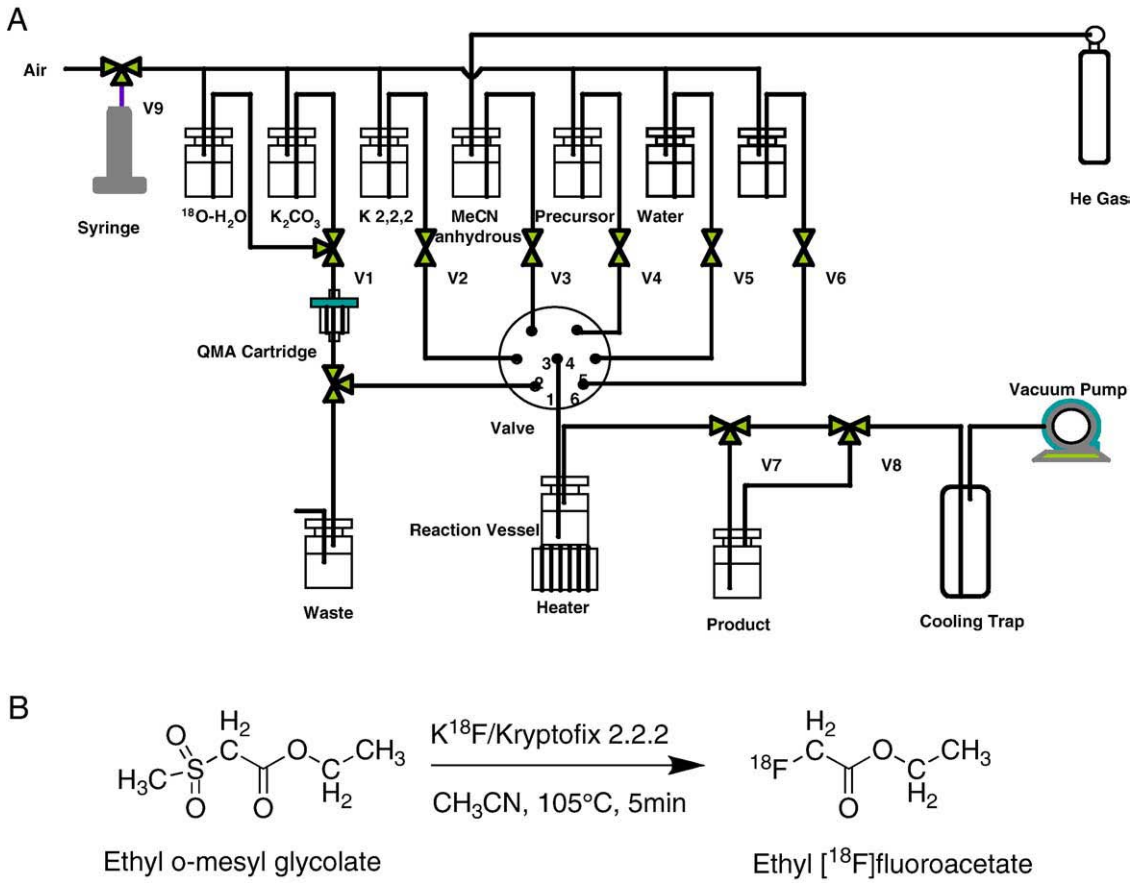

Fig. 2. (A) Diagram of a simple instrument for the preparation of [^{18}F]EFA. (B) Scheme of [^{18}F]EFA synthesis.

2.3. Brain permeability studies of [^{14}C]EFA

The brain uptakes of [^{14}C]EFA and sodium [^{14}C]FA were estimated by the brain uptake index (BUI) method [24]. Male Wistar rats weighing 230–250 g (n=4) were anaesthetized using sodium pentobarbital (35 mg/kg ip), and their right carotid arteries were surgically exposed. Saline solution (0.1 ml) containing 37 kBq of carbon-14-labeled compound and 37 kBq of [^{3}H]water was injected via the carotid artery. At 20 s after injection, the rat was decapitated, and its brain was removed. The right cortex was weighed (50 mg), then 1 ml of Soluene (Perkin-Elmer, Inc., Waltham, MA, USA) was added for liquefaction. After 1 h of incubation at 60°C, 9 ml of cocktail was added to the sample, and radioactivity was counted in a liquid scintillation counter (Packard Instruments Co., VA, USA). The BUI was calculated according to Eq. (1):

$$\mathrm{BUI}(\%) = \frac{\left[{}^{14}\mathrm{C}\text{ in the right cortex}\right]/\left[{}^{3}\mathrm{H}\text{ in the right cortex}\right]}{\left[{}^{14}\mathrm{C}\text{ injected }\right]/\left[{}^{3}\mathrm{H}\text{ injected}\right]} \times 100 \quad (1)$$

2.4. Hydrolysis studies in rat brain

Male Wistar rats (n=3) were anaesthetized with an intraperitoneal injection of sodium pentobarbital, and a carotid artery was surgically exposed. [^{14}C]EFA (37 kBq) in 0.1 ml of saline was injected via the carotid artery, and the rat was decapitated at 5 min after the injection. The cerebral cortex (50 mg) was homogenized in 0.5 ml of ice-cold 10 mM Tris–HCl buffer (pH 7.4) containing 0.25 M sucrose and extracted with 0.5 ml of ethyl acetate. The radioactivities of the lipophilic and water fractions were counted by a liquid scintillation counter. The percentage of radioactivity in the lipophilic fraction was calculated by dividing the radioactivity in the lipophilic fraction by the sum of both fractions, as shown in Eq. (2):

$$\%\text{ of }14\mathrm{C}\text{ in lipophilic fraction} = \frac{14\mathrm{C}\text{ in lipophilic fraction}}{14\mathrm{C}\text{ in lipophilic fraction} + 14\mathrm{C}\text{ in water fraction}} \times 100 \quad (2)$$

2.5. Stability studies in the plasma of several animal species

The hydrolysis of radiolabeled EFA in the plasma was investigated using five animal species, namely, rat, rabbit, dog, common marmoset and human (n=3, respectively). Each plasma sample (200 μl) was incubated with [^{14}C]EFA (370 Bq/10 μl in ethanol) at 37°C in a 1.5-ml microcentrifuge tube. After 5, 10, 30 and 60 min, the hydrolysis reactions were stopped by adding ice-cold water-saturated ethyl acetate (200 μl). The mixture was vortexed and centrifuged at 14,000 rpm for 1 min. The ethyl acetate fraction of the intact form and the water fraction of hydrolyzed metabolites were collected (50 μl), respectively. The radioactivity in each fraction was counted by a liquid scintillation counter. All incubations were performed in triplicate. The percentage of radioactivity in the lipophilic fraction was calculated in Eq. (2).

2.6. Biodistribution studies in ddY mice

Biodistribution studies of [^{18}F]EFA and [^{18}F]FA were carried out using 7-week-old ddY mice. Each compound (37 kBq) was intravenously injected and sacrificed at 30, 60 and 90 min postinjection (n=3-4 per time point). Samples of blood, brain, heart, liver, bone and muscle were removed and weighed. Their radioactivity was counted in an Aloka ARC-380 well scintillation counter (Aloka, Tokyo, Japan). All data were corrected for ^{18}F decay and reported as percent injected dose per gram of tissue (%ID/g ± S.D.)

2.7. PET imaging studies in common marmosets

PET imaging studies were performed with an ADVANCE system (General Electric Medical System, Milwaukee, WI). The physical characteristics of this scanner have been described in detail by DeGrado et al. [25]. A standard pin source of ^{68}Ge/^{68}Ga was used for attenuation corrections of emission images. Common marmoset was anesthetized with a ketamine–xylazine cocktail (20 and 3 mg/kg im, respectively) and sodium pentobarbital (20 mg/kg ip) [26]. [^{18}F]EFA (11.9–12.6 MBq; n=3) or [^{18}F]FA (13.8 MBq; n=1) was injected via a saphenous vein. PET scanning was performed for 90 min with 12 frames at 10-s intervals, 8 frames at 1 min, 4 frames at 5 min, and 6 frames at 10 min. After the scanning, a 6-mm circular region of interest (ROI) was placed on transaxial PET images at the area of the highest accumulated radioactivity of [^{18}F]EFA in the brain. The ROI for [^{18}F]FA was placed on the same area of [^{18}F]EFA. The percent injected dose per gram of ROI (%ID/g) for time–activity curves was calculated using Eq. (3). In Eq. (3), a calibration factor was applied to these ROI data:

$$\%\mathrm{ID/g} = \frac{\text{tissue radioactivity concentration (MBq/ml)}}{\text{injection dose (MBq)}} \times \frac{\text{tissue volume (ml)}}{\text{body weight (g)}} \times 100 \quad (3)$$

2.8. Metabolite studies of [^{18}F]EFA in nonhuman primate

Common marmosets (n=2) were anesthetized, and [^{18}F]EFA was injected via a saphenous vein. At 1 h after administration, the marmoset was euthanized, and arterial blood and selected organs (namely, brain, heart, lungs, liver and kidneys) were collected. The organs were homogenized by a polytron homogenizer with 10 times volume of ice-cold methanol and then centrifuged at 15,000 rpm for 10 min. The supernatants thus obtained were spotted on a TLC plate and developed with standards, namely, [^{18}F]EFA, [^{18}F]FA, [^{14}C]citrate, [^{14}C]acetyl-CoA and [^{18}F]NaF, using the following

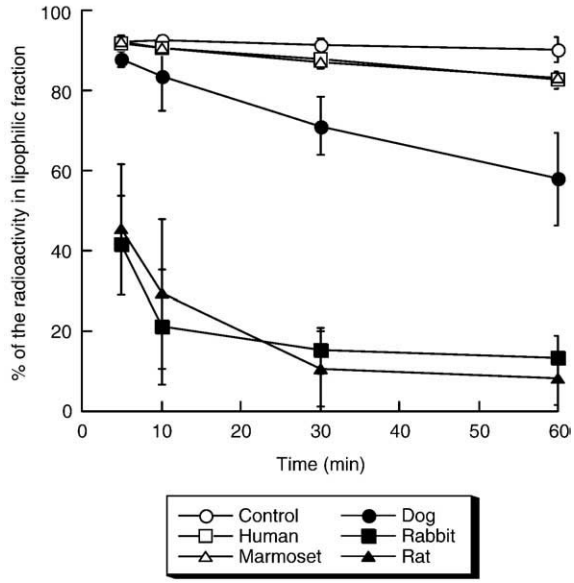

Fig. 3. The percentage of intact [^{14}C]EFA against time in the plasma of five animal species.

solutions: (a) chloroform/methanol (1:1) and (b) diethyl ether/formic acid/water (3:1:1). The former condition could separate [^{18}F]EFA (R_f=0.9), [^{18}F]FA (R_f=0.7) and others (R_f=0). The latter one distinguished among [^{14}C]citrate (R_f=0.3), [^{14}C]acetyl-CoA (R_f=0) and others (R_f=0.9). [^{14}C]citrate and [^{14}C]acetyl-CoA were used as standards to determine [^{18}F]fluorocitrate and [^{18}F]fluoroacetyl-CoA, respectively. Metabolites were detected using a Fuji Photo Film BAS-1500 imaging analyzer (Fuji, Tokyo, Japan) and identified by comparison with standards.

3. Results

3.1. Synthesis of [^{18}F]EFA

[^{18}F]EFA was obtained from ethanol solution with a yield of 28.6±3.6% (n=11). Radiochemical purity was determined to be up to 95%, and synthesis time was 29 min. The stability of [^{18}F]EFA was confirmed after 6 h.

3.2. Brain permeability studies of [^{14}C]EFA

Brain permeability was estimated by the BUI method using ^{14}C compounds and [^{3}H]H_2O. The BUIs of [^{14}C]EFA and [^{14}C]FA were 125.9±4.1% and 33.3±3.7%, respectively (n=4). These data show that the BUI of [^{14}C]EFA was 3.8 times higher than that of [^{14}C]FA.

3.3. Hydrolysis studies in rat brain

In vivo hydrolysis of [^{14}C]EFA was estimated using rat brain. The percentage of radioactivity in lipophilic and water fractions was calculated after extraction from the cerebral cortex. The percentage of radioactivity in the lipophilic fraction representing the intact [^{14}C]EFA was 3.5±3.0% of the total radioactivity at 5 min after injection (n=3).

3.4. Stability studies in the plasma of several animal species

The stability of radiolabeled EFA in plasma was investigated using several animal species. The time courses of the intact [^{14}C]EFA in plasma are given in Fig. 3. In both rat and rabbit plasma, [^{14}C]EFA was hydrolyzed quickly, and less than 21% of the radioactivity was found in the lipophilic fraction at 30 min. Dog plasma showed a gradual degradation curve, and about 58% of the radioactivity was extracted in lipophilic fraction at 60 min. In primates (namely, marmosets and humans), over 80% of the radioactivity was found in the lipophilic fraction at 60 min.

3.5. Biodistribution studies in ddY mice

The biodistribution of [^{18}F]EFA and [^{18}F]FA was carried out in ddY mice. Table 1 displays the percent injected dose per gram of tissue (%ID/g ± S.D.) of selected organs at 30, 60 and 90 min after injection. Intense activities were found in the blood, heart and lungs in [^{18}F]EFA and [^{18}F]FA. We also confirmed brain uptake in both tracers, and the %ID/g value of [^{18}F]EFA was higher than that of [^{18}F]FA at 30 min (6.88±0.53%ID/g vs. 4.97±0.38% ID/g, respectively; P=0.001). In the case of [^{18}F]FA, slow clearance from the brain was observed from 30 to 90 min (4.97±0.38%ID/g and 4.05±0.22%ID/g, respectively; P=0.006); however, the activity in the brain did not change

Table 1
Biodistribution data of [^{18}F]EFA and [^{18}F]FA in ddY mice (n=3 or 4)

Organ	[^{18}F]EFA (%ID/g±S.D.)			[^{18}F]FA (%ID/g±S.D.)		
	30 min	60 min	90 min	30 min	60 min	90 min
Blood	10.88±0.62**	9.46±0.80**	8.51±0.49**	7.10±0.72	7.46±0.33	6.08±0.47
Brain	6.88±0.53**	6.41±0.39*	6.37±0.11**	4.97±0.38	5.13±0.55	4.05±0.22
Heart	10.66±1.67**	10.92±1.17**	8.93±1.64*	6.12±1.08	7.56±0.84	5.93±0.80
Lungs	9.94±1.14**	8.63±0.53**	7.94±0.35**	5.70±0.88	6.17±0.31	5.22±0.49
Liver	8.42±0.36**	7.48±0.29**	9.04±3.44*	5.37±0.54	5.49±0.54	4.61±0.64
Bone	8.55±1.16*	10.66±2.71	11.42±3.85	4.64±1.78	10.27±2.60	8.22±2.25
Brain/blood ratio	0.63±0.03	0.68±0.05	0.75±0.06	0.70±0.04	0.69±0.06	0.67±0.03

* P<0.05 compared with [^{18}F]FA data in the corresponding tissue.
** P<0.01 compared with [^{18}F]FA data in the corresponding tissue.

from 30 to 90 min in [^{18}F]EFA (6.88±0.53%ID/g and 6.37±0.11%ID/g, respectively; *P*=ns). The radioactivity in the bone, indicating defluorination, increased significantly over time following the administration of both compounds.

3.6. PET studies of [^{18}F]EFA and [^{18}F]FA

A brain PET image of [^{18}F]EFA and [^{18}F]FA in a common marmoset is shown in Fig. 4A. The time–activity curves of ROIs for [^{18}F]EFA and [^{18}F]FA in the brain are shown in Fig. 4B. The radioactivity of [^{18}F]EFA in the brain increased to 0.29±0.07%ID/g at 3 min after injection and then decreased gradually up to 10 min. After that, the radioactivity was retained until 90 min, and the %ID/g value was higher than that of [^{18}F]FA (0.22±0.03%ID/g vs. 0.18% ID/g at 60 min, and 0.21±0.03%ID/g vs. 0.17%ID/g at 90 min, respectively).

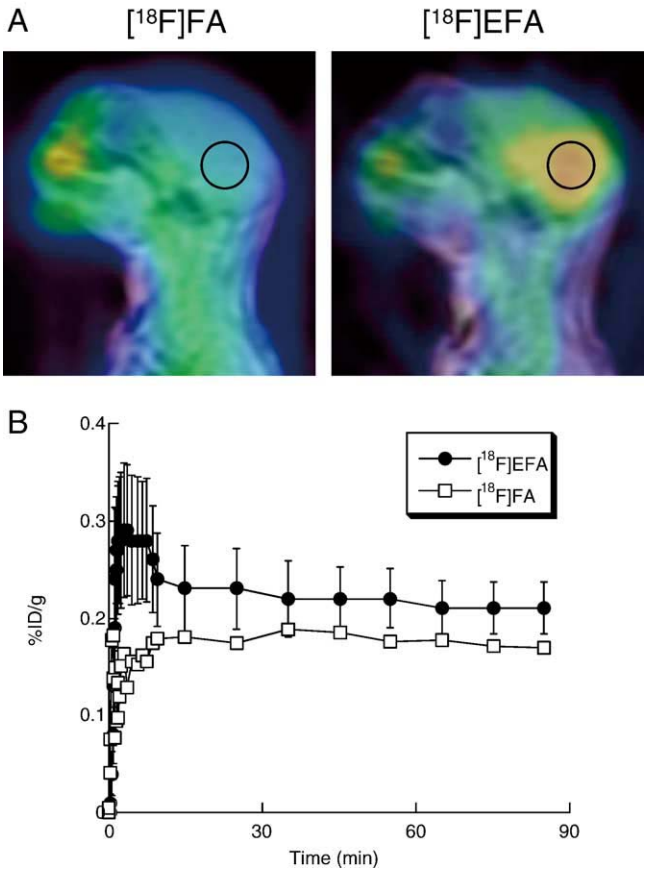

Fig. 4. (A) Dynamic brain PET images of [^{18}F]FA (left) and [^{18}F]EFA (right) (0–10 min) in nonhuman primate. The images are fused to T_1-weighted magnetic resonance images. ROI in the brain set in the black circle. (B) Time–activity curves of [^{18}F]EFA-PET (*n*=3) and [^{18}F]FA-PET (*n*=1) in common marmoset. The values for [^{18}F]EFA are given as mean±S.D. from three animals. Common marmoset was anesthetized with a ketamine–xylazine cocktail (20 and 3 mg/kg im, respectively) and sodium pentobarbital (20 mg/kg ip). [^{18}F]EFA (11.9–12.6 MBq; *n*=3) or [^{18}F]FA (13.8 MBq; *n*=1) was injected via a saphenous vein. PET scanning was performed for 90 min with 12 frames at 10-s intervals, 8 frames at 1 min, 4 frames at 5 min, and 6 frames at 10 min.

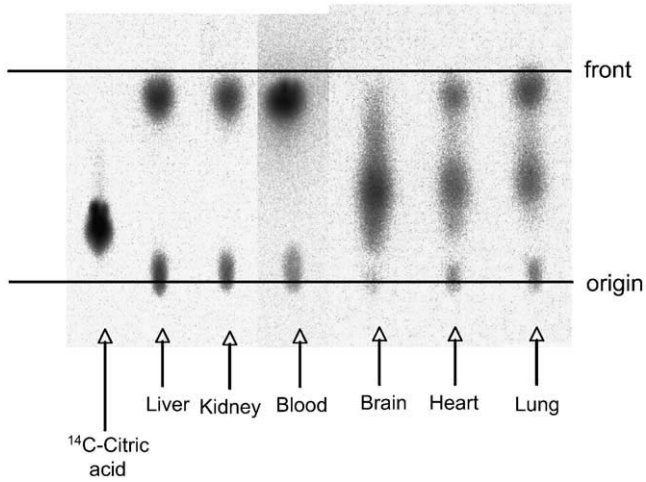

Fig. 5. Radio-TLC analysis of the metabolites in common marmoset at 1 h after injection of [^{18}F]EFA (Solvent B). The R_f values at this condition are as follows: [^{18}F]EFA: 0.9; [^{18}F]FA: 0.9; [^{14}C]citrate: 0.3; [^{14}C]acetyl-CoA: 0.0; [^{18}F]NaF: 0.9.

3.7. Metabolites in marmosets

Fig. 5 shows the radio-TLC of metabolites in typical organs. The metabolites in the whole blood, liver and kidneys at 1 h after administration were only [^{18}F]FA, but unidentified metabolites were detected near the [^{14}C]citrate's R_f value in the brain, heart and lungs.

4. Discussion

We selected [^{18}F]EFA, instead of radiolabeled acetate, as an imaging tracer for glial metabolism in view of the membrane permeability and characteristics of ester compounds. This ester is considered to offer high membrane permeability, and ethanol is safe to tissues after the hydrolysis of acetate ester.

The synthesis of [^{18}F]EFA was performed by a facile method via distillation on a simple instrument set-up. The instrument did not need special parts and could be assembled in any chemical laboratory. This synthesis might be performed anywhere even without an automatic synthesizer. As [^{18}F]EFA is not stable in aqueous solution, we attempted to trap it with pure ethanol in distillation. At the same time, ethanol was cooled by ice water. Before use in animal experiments, the ethanol solution might immediately be diluted by saline. This procedure offers a good way of providing a high concentration of [^{18}F]EFA at the time of injection.

The BUI studies revealed that radiolabeled EFA has high BBB permeability, the value being 3.8 times higher than that of FA. This result suggested that our strategy was appropriate in view of the BBB permeability. To evaluate our proradiotracer concept, the percentage of intact [^{14}C]EFA was calculated. The result showed that the intact [^{14}C]EFA was 3.5±3.0% in the rat cortex at 5 min after injection. It is suggested that [^{14}C]EFA was hydrolyzed rapidly in the brain

and that EFA functioned as a proradiotracer based on our strategy. However, it is known that esterase activity in the blood varies considerably among animal species [27–30], so the stability of EFA was assessed in the plasma of five animal species. These experiments demonstrated that [^{14}C]EFA was hydrolyzed instantly in rodent plasma; however, it was stable in primate plasma (Fig. 3).

The biodistribution studies in mice were carried out to compare tissue uptake and clearance between [^{18}F]EFA and [^{18}F]FA. The uptake of [^{18}F]EFA in the brain demonstrated retention in the brain and faster clearance in the blood at 30 and 90 min after injection, compared to [^{18}F]FA. This may be due to the difference in lipophilicity of the two tracers, and [^{18}F]EFA would be available for delayed brain imaging. The uptakes of [^{18}F]EFA in the heart and lungs were also high. These high uptakes suggest that [^{18}F]EFA may also be useful for myocardial and pulmonary perfusion imaging. Intense accumulation in the bone, which indicates defluorination, was observed over time in both tracers. We believe that the defluorination was derived from [^{18}F]FA because Ponde et al. [31] reported that [^{18}F]FA was rapidly decomposed in rodents. In these biodistribution studies, we found differences in in vivo behavior between the two tracers. However, we were unable to disregard two points as follows: the difference in the ester stability and defluorination of [^{18}F]FA between animal species. In the former point, we confirmed that [^{14}C]EFA was more stable in primate plasma than in rodent plasma. In the latter, Ponde et al. [31] also reported that [^{18}F]FA was stable in primates for 2 h. Therefore, we performed PET and metabolism studies using nonhuman primate (namely, common marmoset) in order to assess [^{18}F]EFA as a proradiotracer for the measurement of glial metabolism.

In nonhuman primate PET studies, a high accumulation of radioactivity in the brain was observed when [^{18}F]EFA was injected (Fig. 4A). The radioactivity in the brain increased to 0.29±0.07%ID/g at 3 min after injection and then decreased quickly to 10 min (Fig. 4B). After 10 min, sufficient radioactivity was retained in the brain. However, the equilibrium in the brain was significantly higher following [^{18}F]EFA administration than following [^{18}F]FA administration, but was not as great as the difference at early time points in the primate. The first uptake until 10 min may represent BBB permeability depending on blood flow, and clearance from the brain may represent competition between the rate of ester hydrolysis and the reverse BBB permeability of [^{18}F]EFA. Furthermore, since the metabolic rate of FA is slow [20], the hydrolyzed [^{18}F]EFA (i.e., [^{18}F]FA) also could gradually clear from the brain. The gradual decrease in radioactivity until about 30 min may represent this condition. After 30 min, the retention may represent the trapped [^{18}F]EFA such as [^{18}F]FA and/or its metabolite in the TCA cycle. These results shows that [^{18}F]EFA could function as a proradiotracer of [^{18}F]FA in nonhuman primate.

We confirmed that the uptake of [^{18}F]EFA in the brain is higher than that of [^{18}F]FA in both primates and rodents. They were normal animals, and so the amount of retention will be different in disease states where glial metabolism is altered. It is highly likely that, due to the greater delivery of [^{18}F]EFA to the brain compared to [^{18}F]FA, the difference in these disease areas will be greater than that in the normal brain.

The metabolism studies in common marmosets revealed that only [^{18}F]FA was detected in the blood, liver and kidney at 1 h after injection, as shown in Fig. 5. Interestingly, metabolites such as [^{18}F]FA and [^{18}F]fluorocitrate were determined in the heart, lungs and brain. These results suggested that the metabolism of [^{18}F]EFA via the TCA cycle in the brain occurred through the oxidative route and was more rapid than that in other organs. It was reported that the metabolites of [^{14}C]FA in rat brains were practically undetectable at 10 min and 1 h [20]. However, metabolites were confirmed at 1 h in primate brains in our experiments. It is known that the symptoms of FA toxicity are different among animal species [32], so the metabolic pattern (metabolic rate, amount, formation and so on) of EFA might be dependent on species. Further studies of metabolites in the brain are required.

5. Conclusion

[^{18}F]EFA rapidly entered the brain and then was hydrolyzed to TCA cycle metabolites in the brains of common marmosets. [^{18}F]EFA is a candidate proradiotracer for the measurement of glial metabolism in the brain, although further studies are required to analyze the metabolites in the brain.

Acknowledgments

Part of this study was supported by the Research and Development Project Aimed at Economic Revitalization from the Ministry of Education, Culture, Sports, Science and Technology Japan, the 21st Century COE program “Biomedical Imaging Technology Integration Program” from the Japan Society for the Promotion of Science, and a grant for Collaboration of Regional Entities for the Advancement of Technological Excellence from the Japan Science and Technology Agency.

References

[1] Bains JS, Oliet SH. Glia: they make your memories stick! Trends Neurosci 2007;30:417–24.
[2] Haydon PG, Carmignoto G. Astrocyte control of synaptic transmission and neurovascular coupling. Physiol Rev 2006;86:1009–31.
[3] Nedergaard M, Ransom B, Goldman SA. New roles for astrocytes: redefining the functional architecture of the brain. Trends Neurosci 2003;26:523–30.
[4] Volterra A, Meldolesi J. Astrocytes, from brain glue to communication elements: the revolution continues. Nat Rev Neurosci 2005;6:626–40.
[5] Haberg A, Qu H, Sonnewald U. Glutamate and GABA metabolism in transient and permanent middle cerebral artery occlusion in rat:

importance of astrocytes for neuronal survival. Neurochem Int 2006; 48:531–40.
[6] Hosoi R, Kashiwagi Y, Tokumura M, Abe K, Hatazawa J, Inoue O. Sensitive reduction in ^{14}C-acetate uptake in a short-term ischemic rat brain. J Stroke Cerebrovasc Dis 2007;16:77–81.
[7] Anezaki T, Yanagisawa K, Takahashi H, Nakajima T, Miyashita K, Ishikawa A, et al. Remote astrocytic response of prefrontal cortex is caused by the lesions in the nucleus basalis of Meynert, but not in the ventral tegmental area. Brain Res 1992;574:63–9.
[8] Hundal O. Major depressive disorder viewed as a dysfunction in astroglial bioenergetics. Med Hypotheses 2007;68:370–7.
[9] Kondziella D, Brenner E, Eyjolfsson EM, Markinhuhta KR, Carlsson ML, Sonnewald U. Glial–neuronal interactions are impaired in the schizophrenia model of repeated MK801 exposure. Neuropsychopharmacology 2006;31:1880–7.
[10] Qu H, Eloqayli H, Muller B, Aasly J, Sonnewald U. Glial–neuronal interactions following kainate injection in rats. Neurochem Int 2003; 42:101–6.
[11] Zwingmann C, Leibfritz D, Hazell AS. Brain energy metabolism in a sub-acute rat model of manganese neurotoxicity: an ex vivo nuclear magnetic resonance study using [1-^{13}C]glucose. Neurotoxicology 2004;25:573–87.
[12] Muir D, Berl S, Clarke DD. Acetate and fluoroacetate as possible markers for glial metabolism in vivo. Brain Res 1986;380:336–40.
[13] Waniewski RA, Martin DL. Preferential utilization of acetate by astrocytes is attributable to transport. J Neurosci 1998;18:5225–33.
[14] Kuge Y, Hikosaka K, Seki K, Ohkura K, Nishijima K, Tsukamoto E, et al. In vitro uptake of [1-^{14}C]octanoate in brain slices of rats: basic studies for assessing [1-^{11}C]octanoate as a PET tracer of glial functions. Nucl Med Biol 2002;29:303–6.
[15] Kuge Y, Kawashima H, Yamazaki S, Hashimoto N, Miyake Y. [1-^{11}C] octanoate as a potential PET tracer for studying glial functions: PET evaluation in rats and cats. Nucl Med Biol 1996;23:1009–12.
[16] Yamazaki S, Fukui K, Kawashima H, Kuge Y, Miyake Y, Kangawa K. Uptake of radioactive octanoate in astrocytoma cells: basic studies for application of [^{11}C]octanoate as a PET tracer. Ann Nucl Med 1996;10: 395–9.
[17] Inoue O, Hosoi R, Momosaki S, Yamamoto K, Amitani M, Yamaguchi M, et al. Evaluation of [^{14}C]phenylacetate as a prototype tracer for the measurement of glial metabolism in the rat brain. Nucl Med Biol 2006; 33:985–9.
[18] Momosaki S, Hosoi R, Sanuki T, Todoroki K, Yamaguchi M, Gee A, et al. [^{14}C]Benzyl acetate is a potential radiotracer for the measurement of glial metabolism in the rat brain. Nucl Med Biol 2007;34:939–44.
[19] Fonnum F, Johnsen A, Hassel B. Use of fluorocitrate and fluoroacetate in the study of brain metabolism. Glia 1997;21:106–13.
[20] Lear JL, Ackermann RF. Evaluation of radiolabeled acetate and fluoroacetate as potential tracers of cerebral oxidative metabolism. Metab Brain Dis 1990;5:45–56.
[21] Hassel B, Bachelard H, Jones P, Fonnum F, Sonnewald U. Trafficking of amino acids between neurons and glia in vivo. Effects of inhibition of glial metabolism by fluoroacetate. J Cereb Blood Flow Metab 1997; 17:1230–8.
[22] Morrison JF, Peters RA. Biochemistry of fluoroacetate poisoning: the effect of fluorocitrate on purified aconitase. Biochem J 1954;58:473–9.
[23] Sun LQ, Mori T, Dence CS, Ponde DE, Welch MJ, Furukawa T, et al. New approach to fully automated synthesis of sodium [^{18}F] fluoroacetate — a simple and fast method using a commercial synthesizer. Nucl Med Biol 2006;33:153–8.
[24] Oldendorf WH. Measurement of brain uptake of radiolabeled substances using a tritiated water internal standard. Brain Res 1970; 24:372–6.
[25] DeGrado TR, Turkington TG, Williams JJ, Stearns CW, Hoffman JM, Coleman RE. Performance characteristics of a whole-body PET scanner. J Nucl Med 1994;35:1398–406.
[26] Saji H, Iida Y, Kawashima H, Ogawa M, Kitamura Y, Mukai T, et al. In vivo imaging of brain dopaminergic neurotransmission system in small animals with high-resolution single photon emission computed tomography. Anal Sci 2003;19:67–71.
[27] Buchwald P. Structure–metabolism relationships: steric effects and the enzymatic hydrolysis of carboxylic esters. Mini Rev Med Chem 2001; 1:101–11.
[28] Ericsson H, Tholander B, Regardh CG. In vitro hydrolysis rate and protein binding of clevidipine, a new ultrashort-acting calcium antagonist metabolised by esterases, in different animal species and man. Eur J Pharm Sci 1999;8:29–37.
[29] Morikawa M, Inoue M, Tsuboi M. Substrate specificity of carboxylesterase (E.C.3.1.1.1) from several animals. Chem Pharm Bull (Tokyo) 1976;24:1661–4.
[30] Quon CY, Mai K, Patil G, Stampfli HF. Species differences in the stereoselective hydrolysis of esmolol by blood esterases. Drug Metab Dispos 1988;16:425–8.
[31] Ponde DE, Dence CS, Oyama N, Kim J, Tai YC, Laforest R, et al. F-Fluoroacetate: a potential acetate analog for prostate tumor imaging — in vivo evaluation of ^{18}F-fluoroacetate versus ^{11}C-acetate. J Nucl Med 2007;48:420–8.
[32] Clarke DD. Fluoroacetate and fluorocitrate: mechanism of action. Neurochem Res 1991;16:1055–8.